

Synthesis and H₂S Gas-Sensing Properties of SnO₂/ZnO Core/Shell Structure

Tran Thi Ngoc Hoa^{1*}, Trinh Minh Ngoc¹, Nguyen Thi Le¹, Nguyen Van Duy²

¹Department of Medical Physics, Hanoi Medical University, Ha Noi, Viet Nam

²International Institute for Materials Science, Hanoi University of Science and Technology, Ha Noi, Vietnam

*Corresponding author email: tranngochoa@hmu.edu.vn

Abstract

In the study, SnO₂/ZnO core/shell nanowires were synthesized through the two-step processes. First, SnO₂-core nanowires were synthesized from Sn powder source at 750 °C by a chemical vapor deposition method (CVD). The ZnO shell was then deposited on SnO₂ nanowires by a DC sputtering method. The morphological and crystal structures of the grown SnO₂/ZnO core/shell nanostructures were investigated by emission scanning electron microscopy (SEM), field-emission scanning electron microscopy (FESEM), and X-ray diffraction (XRD). The results indicated a successful synthesis of the SnO₂/ZnO core/shell nanowires with the thickness of the ZnO shell ranging from 5 nm, 10 nm, and 15 nm. The H₂S gas sensing properties of the SnO₂/ZnO core/shell structure sensors were then investigated, and results pointed out that the sample with a shell thickness of 10 nm showed an effective response and recovery to H₂S gas in the concentration range 0.25 ppm - 2.5 ppm at the temperature range of 300 °C, 350 °C, 400 °C. The optimal working temperature of the sensor was found at 350 °C, where the sensor has a response of 7.8 towards 2.5 ppm. The selectivity of the sensor at 350 °C was also studied. These findings suggest that the sensor could have potential applications in detecting traces of H₂S gas in the medical, food, and environmental fields.

Keywords: SnO₂/ZnO core/shell structure, thermal evaporation, DC sputtering, sensors.

1. Introduction

Hydrogen sulfide (H₂S) is a colorless gas with a characteristic of a “rotten egg” odor. H₂S is a reducing, corrosive, and very toxic gas. Most of the H₂S gas in the environment has natural origins. As a product of the process of microbial decomposition of organic matter even under hypoxic conditions. Therefore, in polluted rivers and lakes, the occurrence of H₂S gas is often in large amounts [1]. The H₂S gas can be rapidly absorbed by the human lungs, causing respiratory, and nervous system diseases and even death depending on concentration and exposure time [2]. Sulfur not only plays a crucial role in the life of organisms, including humans, but it can also have toxic effects on health and the environment. Human physiology studies have shown that four types of amino acids contain sulfur, and two of them form the protein organization. Clinical research in the human body can help to detect inflammatory diseases, blood clots, visceral pain, cancer, and other health issues [3]. In livestock poultry and aquaculture, controlling the concentrations of sulfur-containing compounds is essential to prevent adverse effects on human health, livestock, and the environment. The generation of livestock production depends on various determinants, including the sulfur-containing compounds in the feed and the biological processes involved in their use. When animals consume sulfur-containing feed, the

sulfur is emitted into the environment as waste. During storage, meat and poultry products undergo an anaerobic decomposition of amino acids, forming sulfur-containing intermediates and volatile sulfur compounds. Therefore, proper control of sulfur content is necessary to increase the value of livestock products and enhance consumers' health. Improper management of sulfur-containing compounds can lead to higher concentrations that negatively impact human health, livestock, and the environment. Moreover, H₂S gas, which is produced during the decomposition of organic matter containing sulfur, including animal waste, can also pose significant risks to human and animal health. Exposure to high concentrations of H₂S gas can cause respiratory and neurological problems, leading to reduced productivity in livestock. H₂S gas emissions also contribute to environmental pollution, leading to adverse effects on air and water quality [4]. Controlling the content will help to increase product value and improve the health of consumers. Therefore, by developing a sensor with a simple fabrication process that can detect at low concentrations, and low power consumption, integrated with mobile devices or wireless networks for identification, accurate analysis of gas at low concentrations will help protect human health and the living environment better [5].

Chemical sensors have many advantages and have been studied and applied to determine the

concentration of H₂S gas. There are several categories of chemical sensing technology based on the properties of fabrication materials and electrical properties, such as electrochemical sensors, optical sensors, conductive polymer sensors, and semiconductor metal oxide sensors [6]. Electrochemical sensors mainly use solid electrolytes for gas sensing, but they have some limitations, such as poor selectivity, short lifetime, and limited operating temperature range [7, 8]. Optical gas sensors based on light absorption and emission have good sensitivity and fast response, but they are complex to design and manufacture, resulting in a high cost and limited applicability. Conductive polymer-based electrochemical sensors have advantages in easy fabrication, low cost, and good sensitivity, but they have some limitations in real environments, as their performance depends heavily on the material's chemical and morphological properties [9].

Gas sensors for civil applications require good sensitivity, high reliability, low manufacturing cost, small size, and low operating power. To be able to satisfy the above requirements, the MOS-based approach seems to be the best candidate so far. In the family of MOS, materials for sensitivity, CuO, SnO₂, and ZnO materials are the most used because of their good response to gas [10]. To further enhance the sensor's gas-sensing, the pure materials have been denatured with different metals [11] or can be decorated with other semiconductor metal oxides [12], because after being denatured by metals, the surface area exposed to the gas of the gas-sensitive material increases, increasing the selectivity and reducing the operating temperature for the sensor. When denatured with other semiconductor metal oxides, heterojunctions are created between the two materials, and at the contact site, potential barriers are created. When this sensor is tested in an environment with gas, the potential barrier will decrease sharply due to the formation of metal-semiconductor junctions [10]. Due to the superiority of other materials, SnO₂ and ZnO have been studied and applied most of all [12]. Therefore, different techniques to create heterojunctions between these two materials are still being researched and developed. The core/shell heterostructure between these two materials helps to take advantage of the heterostructured gas sensor, because they are cheaper than other materials. In the form of a core/shell structure, the contact area between the two materials will increase, enhancing the gas-sensitive properties compared to pure materials. If a simple manufacturing method can be used to fabricate a sensor with a core/shell structure of SnO₂/ZnO, it would be very significant [10].

In this study, we developed a SnO₂/ZnO core/shell nanowire gas sensor for detecting H₂S. The sensor was fabricated using a two-step process. First, we fabricated the core SnO₂ nanowires using the CVD

method with tin metal powder as the source material. Next, we used the sputtering method to fabricate the ZnO shell material, and the thickness of the shell was controlled by varying the sputtering time. The gas characteristic of the core/shell sensors depends on the thickness of the shell layer. Our results showed that the SnO₂/ZnO core/shell nanowire gas sensor with a shell thickness of 10 nm had the best sensitivity to gas at a concentration of 0.25 ppm.

2. Experiment

The sensor with SnO₂/ZnO core/shell structure was fabricated in two steps. In the first step, the SnO₂ nanowires network is fabricated by the CVD method, the source material is a metal tin powder with 99.9% purity. The SnO₂ nanowires network is fabricated directly on the digits integrated electrodes, as shown in Fig. 1a. Take approximately 0.1 grams of pure tin powder (Merck, 99.9%) into the quartz boat, then position the electrode on the surface of the boat. Afterward, insert the boat into the quartz tube placed at the center of a horizontal furnace. The entire system was firstly purged with Ar with a flow rate of 300 sccm for 5 min to remove steam and impurities. The heat increased at the rate of 36 °C/min from room temperature to 750 °C, which took about 20 minutes. The temperature was kept constant at 750 °C for 15 minutes. During the growth process, we added O₂ gas to the quartz tube at a rate of 0.5 sccm while maintaining the pressure inside the tube at 1.8 x 10⁻² torr. After the CVD growth step, the furnace was naturally cooled down to room temperature. Fig. 1b describes the SnO₂ nanowires network and the conductive channel after the CVD fabrication process.

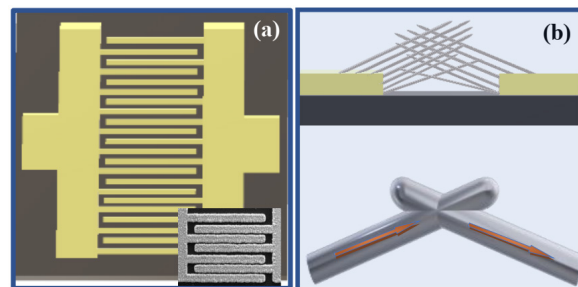


Fig. 1. (a) The digits integrated electrode, (b) SnO₂ nanowires network and conductive channel after the junction

In the second step, the ZnO shell was fabricated by direct deposition onto the surface of SnO₂ nanowires by a sputtering method using a purity Zn target. During the sputtering process, O₂ gas and Ar gas flows were continuously supplied with a flow quantity was 15 sccm (Air Liquide Vietnam, 99.99%). The sputtering power was 50 W, and the thickness of the ZnO layer investigated was 5, 10, and 15 nm, corresponding to sensors SZ5, SZ10, and SZ15, respectively. Finally, the sensors were annealed at 600 °C for 5 h to stabilize the contacts and crystal structure.

The morphology and crystal structure of the fabricated materials were studied by field emission scanning electron microscopy (FESEM, Hitachi S-4800), X-ray diffraction (XRD, Bruker, D5005), and high-resolution transmission electron microscopy (HRTEM, JEOL, JEM-2100). The system for measuring the gas sensitivity of the sensor and how to generate different concentrations of the test gases to be measured has been reported previously [13]. The response of the sensor is studied through the change of resistance, the response (S) of the sensor is defined as the ratio of the resistance in the air (R_a) and the resistance in the gas under investigation (R_g), $S = R_a/R_g$. The temperature for studying the gas sensitivity of the sensor was 300 °C, 350 °C, and 400 °C. The gases selected to investigate the selectivity of the sensor were NH_3 , H_2 , and CO .

3. Results and Discussion

Fig. 2 (a, b) is the SEM image of the fabricated SnO_2 nanowires by the CVD method. Fig. 2a shows that the gas sensors fabricated by the on-chip have the SnO_2 nanowires grown only on the digits of the electrode but not on the SiO_2 substrate. In the inset of Fig. 2a, it is possible to distinguish the silicon substrate and the electrode part that has grown SnO_2 nanowires. The nanowires are grown from two digits that have come into contact with each other. The density of the SnO_2 nanowires is also not too thick, which allows the test gas to be to diffuse to the nanowires below. The average SnO_2 nanowires diameter is about 50 nm, and their surfaces are quite smooth.

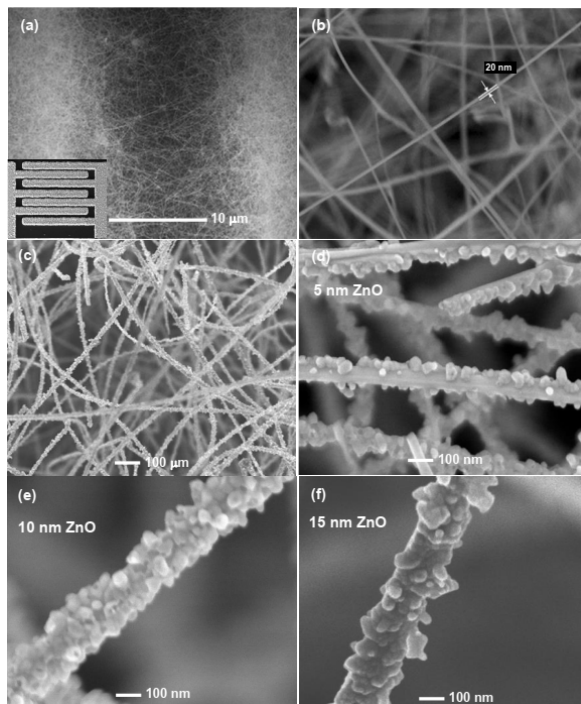


Fig. 2. SEM images of pure SnO_2 nanowires (a, b), SnO_2 nanowires after sputtering the ZnO shell (c), the ZnO layer SZ5 (d), SZ10 nm (e), SZ15 nm (f)

The gas characteristic of the core/shell sensors depends on the thickness of the shell layer. By controlling the sputtering time, we get different thicknesses of the ZnO layer as shown in Fig. 2(c-f). We can observe that the ZnO shell layer is quite rough because it is formed by particles of different sizes, the diameter of the particles ranges from 5 nm to 50 nm. Thus, with the same fabrication conditions (a sensor), the shell layer will have different thicknesses on all the nanowires. In Fig. 2c, we can see that the ZnO shell layer has sputtered onto the SnO_2 nanowire network, quite evenly across the entire surface, as well as from the top down to the nanowires below.

Fig. 2d shows the result of the sputtering process that formed a ZnO shell in 50 seconds. The ZnO nanoparticles have varied sizes but the small particles are gathered as clusters with 5 nm thickness. In this fabrication condition, the sputtering time is short, so the Zn atoms from the source target adhere to the surface of the SnO_2 nanowires randomly, leading to the inability to completely cover the surface of the SnO_2 nanowires. Moreover, after being annealed, the ZnO layer was clustered into plaques on the surface of the SnO_2 nanowires, so part of the surface of the SnO_2 nanowires was exposed which could have an impact on the overall performance and functionality of the material.

Fig. 2e displays the result of the fabrication of a ZnO layer with a sputtering time of 120 seconds. Upon inspection, it can be seen that the SnO_2 nanowires are completely coated with ZnO nanoparticles of relatively uniform size. However, the surface of the nanowire remains rough. Fig. 2f displays the result with a sputtering time of 200 seconds (SZ15). The surface of the ZnO shell layer is smoother than in the previous condition. Additionally, there are more layer present compared to the result with a sputtering time of 120 seconds (SZ10) and 50 seconds (SZ5). This is because the ZnO shell layer is thicker, leading to the ZnO shell layer differences after annealing [14].

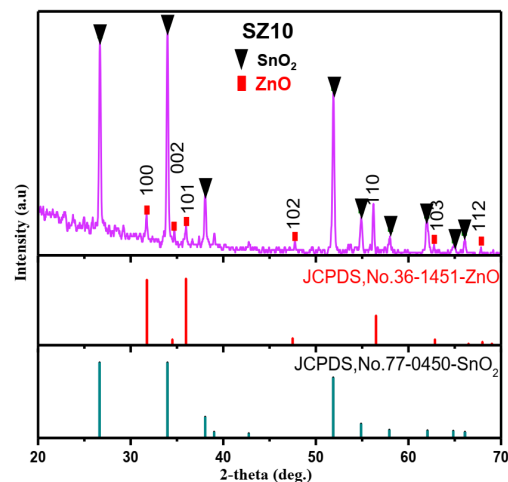


Fig. 3. XRD patterns of the SZ10 sensor

X-ray diffraction (XRD) analysis was conducted to investigate the structural properties of the synthesized materials. The XRD pattern of samples with a 10 nm thick ZnO shell layer (SZ10 sensor) was studied to determine the crystal structure of the materials. As shown in Fig. 3, the SnO₂/ZnO core/shell material sample exhibits the diffraction peaks of the hexagonal ZnO crystal (JCPDS 36-1451) and the tetragonal SnO₂ crystal (JCPDS 41-1445). The ZnO shell displays characteristic peaks for the (100), (002), and (101) faces.

HRTEM images were also studied in Fig. 4 (a-c) to better clarify the microstructure of core/shell materials. Fig. 4a is an HRTEM image of the selected region with a yellow border in the inset image, which shows that there are different lattice fringes at different positions. Focusing on analyzing two locations with crystal fringes, the blue border region, and the red border region, we get the results as shown in Fig. 4b and Fig. 4c. By measuring the distance between the two parallel lattice faces of the crystal, it is possible to determine whether the crystal is SnO₂ or ZnO. The distance between the two lattice faces is 0.28 nm (Fig. 4b) and 0.33 nm (Fig. 4c), respectively, which correspond to the distance between the (001) crystal planes of the hexagonal ZnO and the (110) crystal plane of the quadrilateral SnO₂. This result is completely consistent with the results obtained from the presented SEM and XRD analysis.

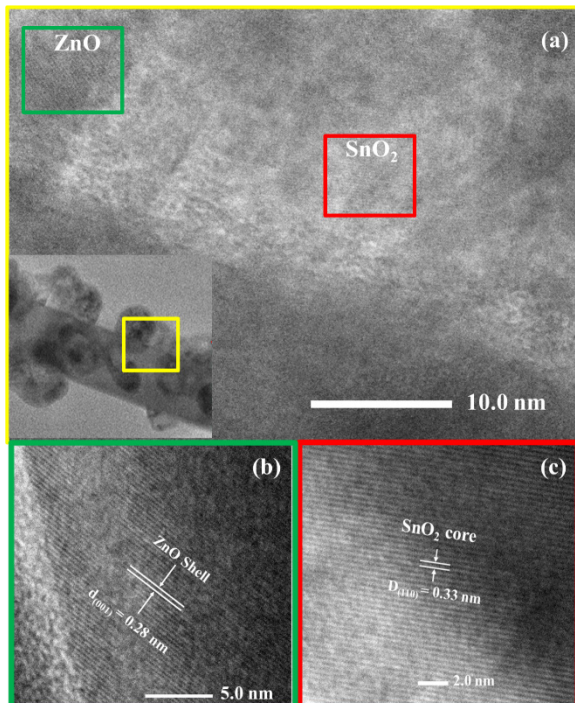


Fig. 4. HRTEM images of SZ10 sensor (a), ZnO crystal (b), and SnO₂ crystal (c)

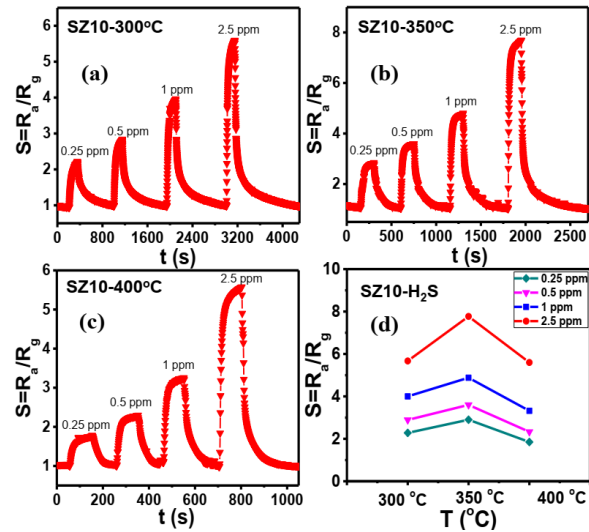


Fig. 5. Transient gas-sensing properties at different concentrations and temperatures (a-c), the response as a function of operating temperature (d)

The temperature selected to investigate the gas-sensing properties of sensors SZ5, SZ10, and SZ15 is 300 °C, 350 °C, and 400 °C. The concentrations selected for the gas-sensitive investigation were 0.25, 0.5, 1, and 2.5 ppm at all temperatures. Fig. 5 (a-c) shows the sensor's response based on SnO₂ networked nanowires sputtered with a 10 nm thick ZnO shell layer (SZ10) and as a function of H₂S concentrations. When the gas concentration increases, the response increases because when the concentration increases, it means that the H₂S molecules that come into contact with the surface of the gas-sensitive material increase, at the investigated temperatures, and the sensor responds and recovers well with gas. Fig. 5d is the response plotted as a function of temperature, the graph shows that the responses have shown a bell-shaped relationship with the investigated temperatures. At the top of the bell shape at 350 °C, the sensor's response increased as the temperature increased from 300 °C to 350 °C and then decreased as the temperature increased to 400 °C. At a working temperature of 350 °C, the response of the SZ10 sensor with 2.5 ppm H₂S gas is the highest (7.8). It can be confirmed that 350 °C is the optimal temperature for the sensor to work.

Considering the response time and recovery time of the sensor with gas as shown in Fig. 6, we show that the response time of the sensor decreases as the operating temperature and concentration increase. With the recovery time of the sensor, when the temperature increases, the recovery time decreases, the concentration of gas increases, and the recovery time increases. The explanations for these are based on the surface reactions of with oxygen adsorbed on the surface of ZnO materials [15]. This result is also consistent with previous publications [16].

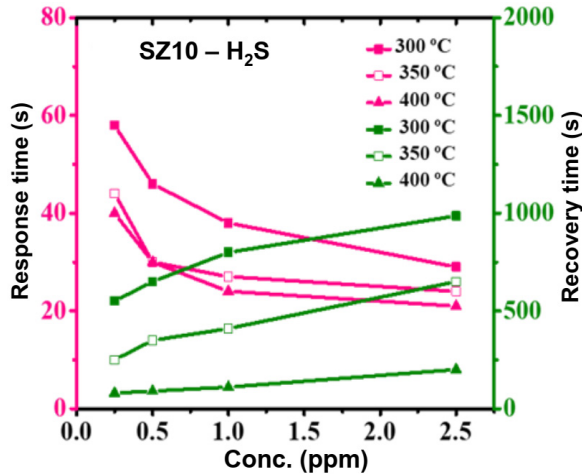


Fig. 6. Response time and recovery time of SZ10 sensor

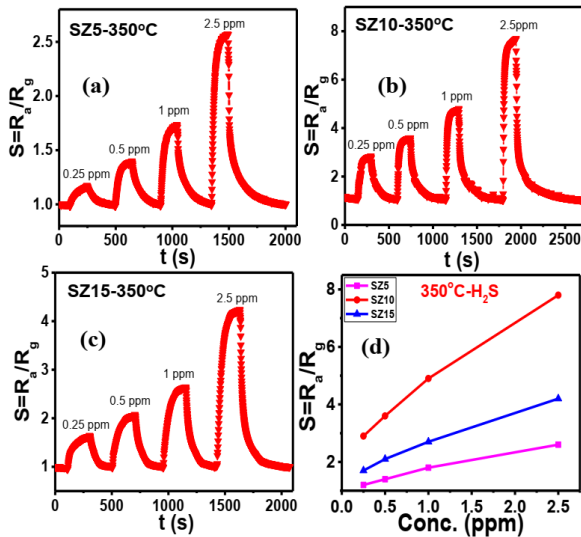


Fig. 7. Comparative results of the responses of SZ5, SZ10, and SZ15 sensors at 350 °C

The study aimed to investigate the impact of the ZnO shell thickness on the gas sensitivity characteristics of the sensors. Three sensors with different ZnO shell thicknesses of SZ5, SZ10, and SZ15 were exposed to H₂S gas at a temperature of 350 °C. The gas response characteristics of these sensors were analyzed and presented in Fig. 7. The findings showed that, for all three sensors, as the gas concentration increased from 0.25 ppm to 2.5 ppm, the response of the sensors increased accordingly (as seen in Fig. 7a-c). However, a comparison between the gas response of the two sensors SZ5 and SZ10 to different concentrations ranging from 0.25 ppm to 2.5 ppm revealed that their response was lower than that of the sensor with the SZ10 sensor at the same concentration range. The response of the sensor with the 10 nm shell layer increased in the range of 2.9 to 7.8 as seen in Fig. 7d. These results confirm that the optimal ZnO shell thickness for the sensor is 10 nm (SZ10).

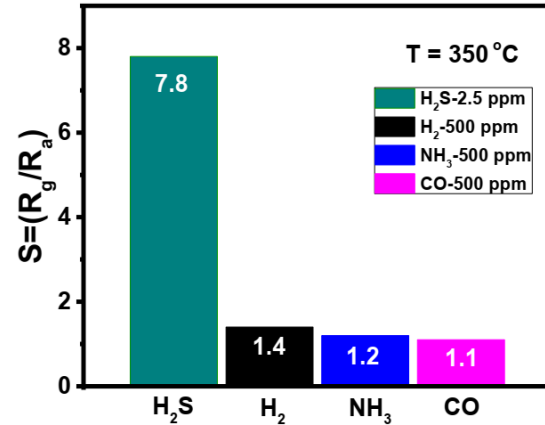


Fig. 8. Selectivity of the SZ10 sensor

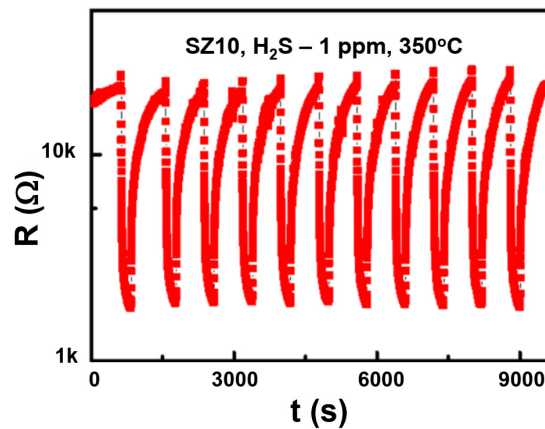


Fig. 9. The stability characteristics of SZ10 sensor

A SnO₂/ZnO core/shell structure sensor with a 10 nm shell layer was utilized in this study to examine its selectivity towards gases H₂, NH₃, and CO at 350 °C. The response results, as depicted in Fig. 8, show that even though the concentration of H₂, NH₃, and CO gases was higher (500 ppm) than the concentration of H₂S gas used in previous tests (2.5 ppm), the response of the sensor was still lower with values of 1.4 (for H₂), 1.2 (for NH₃), and 1.1 (for CO) compared to the response of 7.8 for H₂S gas. This demonstrates that the SnO₂/ZnO core/shell structure sensor operating at 350 °C has excellent selectivity towards these gases, indicating its potential for practical applications.

The short-term stability of the SZ10 sensor has been studied at an operating temperature of 350 °C. Repeated responses to 1 ppm for 10 consecutive measurement cycles did not change significantly (Fig. 9), indicating good short-term stability.

The gas-sensitivity mechanism of the SnO₂/ZnO core/shell sensor structure is shown in Fig. 10. Both SnO₂ and ZnO are two *n*-type semiconductor metal oxides, and SnO₂ has a band gap energy of 3.6 eV, the work function is 4.9 eV, ZnO has a band gap energy of 3.37 eV and the work function is 5.2 eV [15,17]. When a ZnO shell layer is formed on the surface of the SnO₂

nanowires, it created *n-n* heterostructure junctions. The electrons diffuse from SnO₂ to ZnO and holes move in the opposite direction. This process creates a potential barrier at the site of the junction to counteract this diffusion process. Simultaneously, on the ZnO shell side, an accumulation region will be created while the SnO₂ core side will form an electron-poor region and the conduction channel will be narrowed, causing the resistance to increase. When in the atmosphere, the oxygen molecules absorbed on the surface of ZnO will take electrons from ZnO to create oxygen ions which also cause the electron depletion region of the surface. When in an environment with gas at this research condition, a chemical reaction will occur between gas and oxygen ions according to (1) and (2) below. Thus, after the reaction, electrons are returned to ZnO thereby reducing the resistance of the sensor [17].

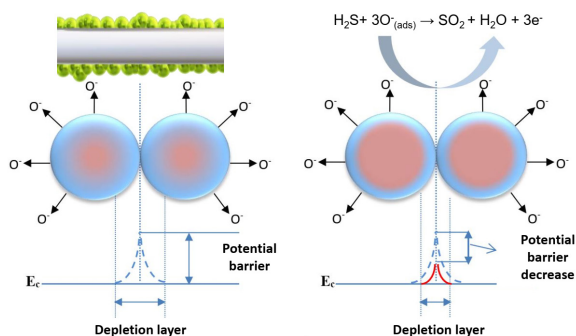
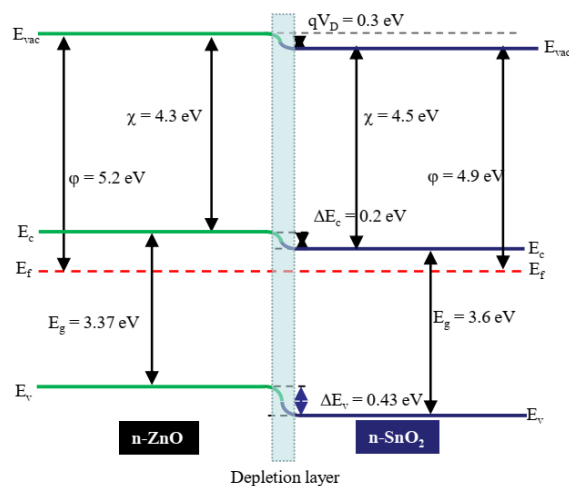
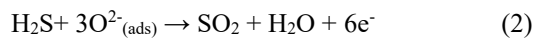
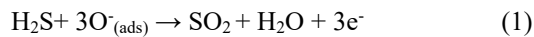


Fig. 10. The diagram presents an explanation of the gas-sensing mechanism of the SnO₂/ZnO core/shell structure

4. Conclusion

We have successfully fabricated a gas sensor with a SnO₂/ZnO core/shell structure using CVD and

sputtering methods. The ZnO shell's thickness strongly influences the sensor's sensitivity to H₂S gas, with the best response observed at a ZnO shell thickness of 10 nm. The optimal operating temperature for the sensor is 350 °C, and it exhibits a response of 7.8 at a gas concentration of 2.5 ppm. The sensor also shows good selectivity to H₂S gas at 350 °C and remains stable for a short time. This study demonstrates the potential application of the sensor in detecting the presence of H₂S gas in the environment.

Acknowledgments

This research is funded by the Vietnamese Ministry of Science and Technology in the Vietnam-Korea joint research program under grant number NĐT/KR/21/20.

References

- [1] Air quality guidelines for Europe. Copenhagen: WHO Regional Office for Europe, WHO Regional Publications, European Series No.23, p. 411, 1987. <https://apps.who.int/iris/handle/10665/107364>
- [2] H. M. Ammann, A new look at physiologic respiratory response to H₂S poisoning, *Journal of Hazardous Materials*, vol. 13, no. 3. pp. 369-374, 1986. [https://doi.org/10.1016/0304-3894\(86\)85008-7](https://doi.org/10.1016/0304-3894(86)85008-7)
- [3] S. Singh and H. Lin, Hydrogen Sulfide in physiology and diseases of the digestive tract, *Microorganisms*, vol. 3, no. 4. pp. 866-889, 2015. <https://doi.org/10.3390/microorganisms3040866>
- [4] K. Saksrithai and A. J King, Controlling hydrogen sulfide emissions during poultry productions, *J. Anim. Res. Nutr.*, vol. 03, no. 01, 2018. <https://doi.org/10.21767/2572-5459.100040>
- [5] S. W. Choi, A. Katoch, J. Zhang, and S. S. Kim, Electrospun nanofibers of CuO-SnO₂ nanocomposite as semiconductor gas sensors for H₂S detection, *Sensors and Actuators, B: Chemical*, vol. 176. pp. 585-591, 2013. <https://doi.org/10.1016/j.snb.2012.09.035>
- [6] A. Stanoiu et al., Sensors based on mesoporous SnO₂-CuWO₄ with high selective sensitivity to H₂S at low operating temperature, *J. Hazard. Mater.*, vol. 331, pp. 150-160, Jun. 2017. <https://doi.org/10.1016/j.jhazmat.2017.02.038>
- [7] X. Liu, S. Cheng, H. Liu, S. Hu, D. Zhang, and H. Ning, A survey on gas sensing technology, *Sensors (Switzerland)*, vol. 12, no. 7, pp. 9635-9665, 2012. <https://doi.org/10.3390/s120709635>
- [8] F. I. M. Ali, F. Awwad, Y. E. Greish, and S. T. Mahmoud, Hydrogen sulfide (H₂S) gas sensor: A Review, *IEEE Sens. J.*, vol. 19, no. 7, pp. 2394-2407, 2019. <https://doi.org/10.1109/JSEN.2018.2886131>
- [9] C. Duc, M. L. Boukhenane, J. L. Wojkiewicz, and N. Redon, Hydrogen sulfide detection by sensors based on conductive polymers: A Review, *Frontiers in Materials*, vol. 7, no. September. 2020. <https://doi.org/10.3389/fmats.2020.00215>

- [10] A. Mirzaei, S. S. Kim, and H. W. Kim, Resistance-based H₂S gas sensors using metal oxide nanostructures: A review of recent advances, *J. Hazard. Mater.*, vol. 357, pp. 314-331, Sep. 2018. <https://doi.org/10.1016/j.jhazmat.2018.06.015>
- [11] J. Ma, Y. Liu, H. Zhang, P. Ai, and N. Gong, Chemical room temperature ppb level H₂S detection of a single Sb-doped SnO₂ nanoribbon device, *Sensors Actuators B. Chem.*, vol. 216, pp. 72-79, 2015. <https://doi.org/10.1016/j.snb.2015.04.025>
- [12] Y. Masuda, Recent advances in SnO₂ nanostructure based gas sensors, *Sensors Actuators B Chem.*, vol. 364, p. 131876, Aug. 2022. <https://doi.org/10.1016/j.snb.2022.131876>
- [13] P. H. Phuoc et al., Comparative study on the gas-sensing performance of ZnO/SnO₂ external and ZnO-SnO₂ internal heterojunctions for ppb H₂S and NO₂ gases detection, *Sensors Actuators B Chem.*, vol. 334, p. 129606, May 2021. <https://doi.org/10.1016/j.snb.2021.129606>
- [14] P. Marwoto, L. Khanifah, Sulhadi, Sugianto, B. Astuti, and E. Wibowo, Influence of annealing time on the morphology and oxygen content of ZnO:Ga thin films, *J. Phys. Conf. Ser.*, vol. 1321, no. 2, p. 022020, Oct. 2019. <https://doi.org/10.1088/1742-6596/1321/2/022020>
- [15] J. Kim and K. Yong, Mechanism study of ZnO nanorod-bundle sensors for H₂S gas sensing, *J. Phys. Chem. C*, vol. 115, no. 15, pp. 7218-7224, 2011. <https://doi.org/10.1021/jp110129f>
- [16] C. Manh, H. Viet, V. Van Thinh, L. Thi, and N. Tat, Sensors and Actuators A : Physical Au doped ZnO / SnO₂ composite nanofibers for enhanced H₂S gas sensing performance, *Sensors Actuators A. Phys.*, vol. 317, p. 112454, 2021. <https://doi.org/10.1016/j.sna.2020.112454>
- [17] J. B. B. R. Prabakaran Shankar, Gas sensing mechanism of metal oxides: The role of ambient atmosphere, type of semiconductor and gases - A review. *p. Sci. Lett. J* (2015) 4 126.